[Frontiers in Bioscience E3, 1013-1024, June 1, 2011]

Development of semiconductor nanomaterial whole cell imaging sensor on glass slides

Hengyi Xu[1,2], Zoraida Pascual Aguilar[2], Hua Wei[1], Andrew Wang[2]

[1]State Key Laboratory of Food Science and Technology, Jiangxi-OAI Joint research institute, Nanchang University, 235 Nanjing Donglu, Nanchang 330047, China, [2]Ocean NanoTech LLC, 2143 Worth Lane, Springdale AR 72764, USA

TABLE OF CONTENTS

1. ABSTRACT

We report the development of a highly specific semiconductor quantum dots (QDs)-based whole cell imaging sensor that offer rapid, reproducible, accurate, and long term cell imaging system on silanized microscope glass slides. The QD-based imaging sensor involved capture of whole cells with QD labeled highly specific antibodies against over expressed cell membrane proteins. The QDs were first modified with a polymer coating to generate carboxyl groups on the surface. Using the carboxylated QDs, antibodies were covalent conjugated using carbodiimide chemistry to form 2^0Ab~QD that were used to capture whole cell. The SK-BR3 cell line was used as a model analyte in the sandwich type assay consisting of 1^0Ab + SK-BR3 + Ab' + 2^0Ab~QD. The assay was immobilized on an antibody modified silanized microscope slide that was subsequently mounted on a fluorescence microscope for detection. The results indicated that the QD based imaging sensor exhibited brighter signals compared with organic dye Texas red. The QD-based whole cell imaging sensor was visible under the microscope even after one week without fixation.

2. INTRODUCTION

Semiconductor quantum dots are now used as a nonspecific fluorescent stain or as specific targeting molecules because of their unique properties. Semiconductor quantum dots are 3-10 nm particles that are made from semiconductor or semiconductor-metal composites (1-3). Quantum dot nanocrystals exhibit high brightness and photostability, that may be exploited for long term staining and observation of cells (4-5). QDs tend to be brighter than organic dyes because of the effects of extinction coefficients that are an order of magnitude larger than those of organic dyes (6-7), comparable quantum yield, and similar emission saturation levels (8). The biggest advantage of QDs resides in their resistance to bleaching over long periods of time (minutes to hours) allowing the acquisition of crisp images over extended periods of time.

Semiconductor QDs have uncomparable advantages that arise out of their unique size-dependent physical properties that include enhanced chemical and photochemical stability (9-11). However, QDs are usually synthesized in organic solvents such as hexane, toluene,

acetone, and/or ethanol (12). In order to be used for biological applications, QDs must first be converted into water-soluble forms to be compatible with biological molecules and tissues.

The most interesting property of QDs for immunofluorescence applications is the very small number of QDs necessary to produce a signal. Indeed, several studies have reported flickering of some specimens, a phenomenon due to the blinking of a small number of QDs (13-14). This demonstrates that single QDs can still be observed especially in immunocytological conditions, with an ultimate sensitivity limit of one QD per target molecule. Additionally, QDs are available in a virtually unlimited number of well-separated colors, all excitable by a single light source. Thus, QDs can be used for multiple analyte imaging detection. Aside from simplifying image acquisition, QDs can be used in confocal microscopy to perform nanometer-resolution colocalization of multiple-color individual QDs (15).

QDs that are used for tagging a biological molecule may be modified with a recognition moiety (e.g., DNA oligonucleotide or aptamer, antibody, etc.) or may be used with a solubilization ligand (16). QD ligands containing either an amine or a carboxyl group can be used for cross-linking molecules containing an N-hydroxysuccinimyl ester moiety (17-18), a thiol group (6, 19-20), or by means of standard bioconjugation reactions. Another approach uses electrostatic interactions between QDs and charged adapter molecules, or between QDs and proteins modified to incorporate charged domains (21). In some studies, streptavidin-coated QDs were used with biotinylated proteins, DNA, or antibodies (17, 22-25). QDs have also been functionalized with streptavidin (22-23), secondary (26) or primary antibodies (24), receptor ligands such as epidermal growth factor (EGF) (27) or serotonin (28), recognition peptides (26), and affinity pairs such as biotin-avidin after engineering of the target protein (17).

Some of the most successful uses of QDs have been in immunofluorescence labeling of fixed cells and tissues; immuno-staining of membrane proteins (19, 23, 27, 29-30), microtubules (23), actin (18, 23), and nuclear antigens (23). QDs have also been used in fluorescence *in situ* hybridization in DNA or chromosomes (14, 31-32).

Non-specific QD-labeling is important for cell counting, cell tracking, or pathogen imaging (6, 33-35). This can be achieved through microinjection (6), electroporation, or phagocytosis of QDs (33-34). Non-specific internalization of QDs was observed in phagokinetic human cancer cells (35) plated on a QD-coated coverslip. It has also been shown to be easily removed by using high concentration of blocking buffers (36-37). For simple determination of the existence of cells, non-specific staining with QDs allows staining that lasts for months (Ocean's unpublished data).

Unlike non-specific staining, specific detection of cells of interest can be achieved efficiently through functionalization of QDs. Functionalized QDs containing specific probes in the form of antibodies or nucleic acids are particularly useful for specific cell or pathogen detection, specific cell tracking, and cell targeting studies (4). This has been shown for mammalian cells (13), bacteria, and yeast cells (33, 38). Currently direct QD functionalization with a secondary antibody involves several methods (26). One approach is cross-linking primary antibodies to QDs for functionalization (33). Another approach involves the biotinylation of the primary antibody, which is subsequently attached to avidin-coated QDs. A third approach involves engineering an adaptor protein with binding affinity to the Fc region of antibodies on one side and electrostatic interactions with charged QDs in another side (21, 33). Researchers have also used ligands of surface receptors bound to QDs via a biotin-streptavidin link (27). QDs coated with natural peptides had also been reported (39). Such QDs exhibited excellent colloidal properties, photophysics, and biocompatibility that can be tailored to provide additional functionalities (40). These studies have shown that QDs have a considerable advantage over standard dyes in that they offer the possibility of long-term observation with negligible photo-bleaching.

Using a simple one step covalent conjugation process for functionalization, we developed a highly specific semiconductor quantum dots (QDs)-based whole cell imaging sensor that offer rapid, sensitive, reproducible, and accurate results. The QD-based imaging sensor was based on the capture of whole cells on silanized microscope glass slides (Figure 1) with QD labeled highly specific antibodies against over expressed proteins on the cell surface. The QDs, that were modified with a polymer coating to generate carboxyl groups on the surface, were covalently conjugated to the antibodies using carbodiimide chemistry to form 2^0Ab~QD. The QD labeled antibodies were used to capture whole human breast cancer cell SK-BR3 (cell) that was used as a model analyte to form 2^0Ab~QD + cell complex. The 2^0Ab~QD + cell complex was captured on an antibody modified silanized microscope slide forming a sandwich type assay consisting of glass slide~aminopropyl triethoxysilane+ 1^0Ab + SK-BR3 + Ab' + 2^0Ab~QD that was subsequently mounted on a fluorescence microscope for detection. The QD based whole cell imaging sensor was visible under the microscope even after one week without fixation.

3. MATERIALS AND METHODS

3.1. Chemicals and reagents

N-(3-dimethylaminopropyl)-n'-ethylcarbodiimide hydrochloride (EDC), n-hydroxysulfosuccinimide sodium salt (sulfo-NHS), and (3-Aminopropyl) triethoxysilane were obtained from Sigma-Aldrich Chemical Corporation (St. Louis, MO). Cell culture medium (RPMI 1640) and antibiotics (streptomycin and penicillin), fetal bovine serum (FBS), Trypsin and Dulbecco's phosphate-buffered saline (DPBS) buffer were obtained from HyClone (Logan, UT). Goat-anti-mouse IgG and Texas red -conjugated goat-anti-mouse IgG (Emission: 620 nm) were purchased from Jackson ImmunoResearch Laboratories (West Grove, PA). Mouse anti-EpCAM IgG, human anti-Her2/Neu human IgG, and anti-mouse IgG (raised in goat and rabbit) were

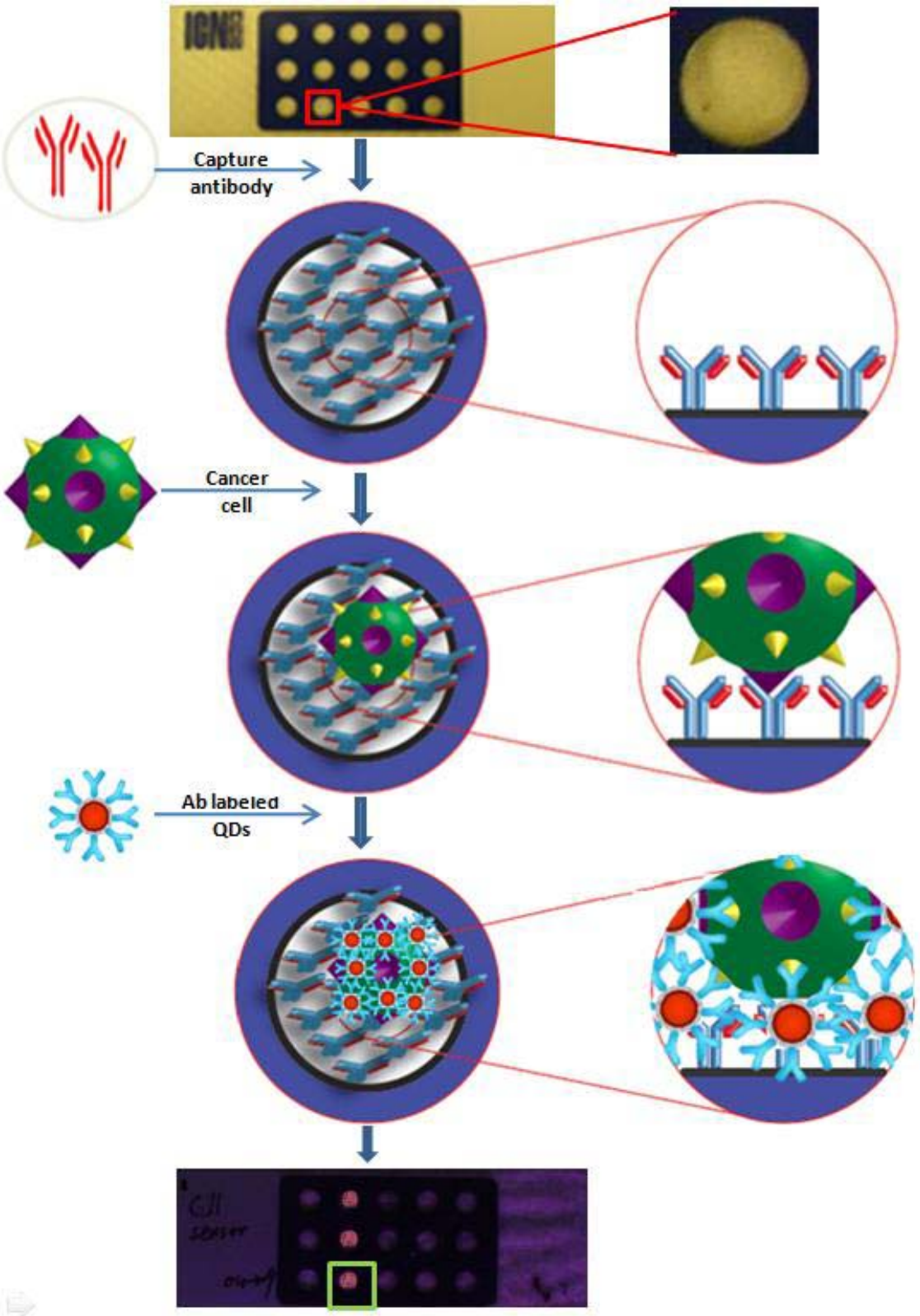

Figure 1. Schematic diagram of the heterogeneous solid platform QDs-based whole cell imaging sensor. Anti-Her2/neu antibody as capture antibody immobilized on the silanized glass slide, anti-EpCAM for labeling, and QD-goat anti-mouse IgG for imaging.

purchased from RayBiotech (Norcross, GA). Water was purified using Millipore Milli-Q water purification system (Billerica, MA).

The water soluble QDs used in all the following studies were commercially available at Ocean NanoTech (Springdale, AR). The QDs were converted to water soluble form through polymer coating that resulted in functionalization with carboxyl groups (Catalog#QSH). The carboxyl groups were used for covalent conjugation to the antibodies.

3.2. Surface modification and bioconjugation of QDs with antibodies

The secondary goat-anti-mouse IgG (antibodies against mouse anti-EpCAM IgG) were conjugated with QDs to form the 2^0Ab~QD. Covalently linked 2^0Ab~QD was prepared using sulfo-NHS and EDC coupling chemistry in a two-step process. The QDs (4 μM) were activated with sulfo-NHS at a molar ratio of 2000:1 and EDC at a molar ratio of 2000:1 for 5 minutes in borate buffer, pH 7.4, to which 2 mg of goat-anti-mouse IgG were added. The mixture was vortexed thoroughly and reacted for 2 h at room temperature. The reaction was stopped by adding 5 μL of quenching buffer (Ocean NanoTech, Springdale, AR) and allowed to react for 10 more minutes. The 2^0Ab~QD conjugates were stored at 4ºC for about 12 h and purified by ultra centrifugation using a Beckman ultracentrifuge (Brea, CA).

3.3. Characterization of QDs and QD-antibody conjugates

The inorganic core size of the QDs was measured using a JEOL (Peabody, MA) transmission electron microscope (TEM). The images were obtained at 100 K magnification at 100 kV using samples prepared by dropping a chloroform solution of QDs onto an agar carbon-coated copper grid (400 meshes) where the solvent was evaporated.

UV-visible absorption spectra were acquired with a Hewlett Packard (HP) 8453 UV-vis absorption spectrophotometer (Palo Alto, CA) and the photoluminescence (PL) spectra were recorded on a Perkin Elmer (PE) Lambda LS 50B luminescence spectrometer (Waltham, MA). The photo luminescence quantum yield (PLQY) was measured using Rhodamine 6G in ethanol as the reference standard (PLQY 95%) (41-42). All optical measurements were performed at room temperature under ambient conditions.

2^0Ab~QD conjugates were evaluated with a Bio-Rad Mini-SubCell GT horizontal submerged gel electrophoresis apparatus (Hercules, CA) using a 1.5% (w/v) agarose gel in Tris-acetate-EDTA (TAE) buffer, pH 8.5. For each well, 10 μL of the QDs or the 2^0Ab~QD conjugates at 100 nM were mixed with 5 μL of 5×TAE loading buffer (5×TAE, 25% (v/v) glycerol at pH 8.5) before loading into the gel. The gel was resolved at 100 V for 30 min with a Bio-Rad PowerPak Basic power supply and then imaged at 2 s exposure using an Alpha Imager HP 2006 gel imaging system (Santa Clara, CA). The hydrodynamic size and zeta potential of the original water soluble QDs and QD~Ab conjugates were measured using Zetatrac dynamic light scattering equipment (York, PA).

3.4. Cell culture

Human breast cancer cell line (SK-BR3) that over-expressed Her2 (43-44) was used as a model analyte for the development of the QD-based whole cell imaging sensor. The cell line SK-BR3 was originally obtained from the American Type Culture Collection (Manassas, VA) and was donated by Dr. Lily Yang from Emory University. SK-BR3 cells were grown in RPMI-1640 medium supplemented with 10% fetal bovine serum (FBS) and 1% of streptomycin/penicillin antibiotics solution. These cultures were placed in a humidified atmosphere at 5% CO_2 at 37°C in a cell culture incubator (Sanyo, Japan). The media were replaced once every three days. The cells were cultured to about 80-90% confluence, and then harvested by adding 1 mL of trypsin for digestion and detachment from the flask. The cells were washed in DPBS buffer and counted to establish the cell concentration under an inverted microscope (Leica, Germany). The cell suspension was adjusted to 100,000 cells/mL with DPBS and stored in 4°C before use in the various experiments. The cells were used within the day of harvest.

3.5. Surface modification of the glass slide used as the capture surface

The capture surface for the QD-based whole cell sensor was a microscope glass slide. The microscope glass slide surface was functionalized with (3-aminopropyl) triethoxysilane before it was used for covalent immobilization of the anti-Her2/neu antibodies. These antibodies specifically targeted the over expressed Her2 proteins on the SK-BR3 cell surface.

To prepare the solid surface for the capture antibody immobilization, the glass slides were soaked overnight in 10% KOH, followed by soaking in 40% 3-aminopropyl) triethoxysilane for 5 h to form self-assembled monolayers of silane. The silanized slides were washed thoroughly with DI water and dried under nitrogen gas. Anti-Her2/neu antibody that targeted the surface of SK-BR3 cells was immobilized on the slides using EDC coupling using the ethoxy group on the silane. Covalent coupling was carried out with 5 μg of antibody mixed with 2 μL of 0.2 M EDC that was placed on the silanized slide surface. The slides were incubated overnight at 4°C and washed thoroughly with autoclaved DI water to remove excess antibody and other reagents. The Her2/neu antibody modified silanized glass slide was used immediately.

3.6. Solid phase quantum dot-based whole cell imaging sensor

The QD-based whole cell imaging sensor was designed using a combination of capture antibody immobilized on the silanized microscope glass slide, cell labeling antibody that targeted the cell surface (that was not bound to the capture platform), and a quantum dot labeled antibody, 2^0Ab~QD that was used for imaging. The primary antibodies, anti-Her2/neu, that were immobilized on the silanized glass slides were used for the specific capture of the cells.

Labeling with antibodies against the epithelial cell adhesion molecules (anti-EpCAM IgG) allowed for the targeting of sites on the cell surface that were not used for capture as well as immobilization of the cells. In this manner, capture of the cell did not interfere with the labeling for subsequent imaging because the target proteins were different. The third antibody that was labeled with QDs to form the 2^0Ab~QD, targeted the mouse anti-EpCAM IgG to form the sandwich type immunoassay for SK-BR3 consisting of 1^0Ab+SK-BR3+Ab'+2^0Ab~QD complex that was immobilized on a glass slide surface shown in Figure 1. Texas-red conjugated goat-anti-mouse IgG (TxRed~2^0Ab) to form the TxRed~2^0Ab + cell complex was used for comparison of the sensitivity and reproducibility of the QD-based whole cell imaging sensor. TxRed~2^0Ab amounts in each assay were calculated based on the antibody number on the 2^0Ab~QD, eg. 1 nM QD~2^0Ab equals 5 μg of TxRed~2^0Ab.

3.7. Optimization of the sensing system

In order to eliminate the non-specific binding of QD-labeled antibody and other proteins on the capture surface, different blocking buffers were tested. The buffers used were as follows: A) PBS based super blocking buffer BBB; B) Tris based super blocking buffer BBG; C) 10 mM Phosphate buffered saline ,PBS, pH 7.4; D) 10 mM Tris-hydroxymethy aminomethane, Tris, pH 7.4; E) 2% Tween in 10 mM PBS, pH 7.4; F) 2% Tween in 10 mM Tris, pH 7.4; G) 0.002% Triton 100X in 10 mM Tris, pH 7.4; H) 2% Triton 100X in 10 mM PBS, pH 7.4; I) 0.002% Triton 100X and 2% Tween in 10 mM PBS, pH 7.4; J) 2% Triton 100X and 2% Tween in 10 mM Tris, pH 7.4; K) Tris-acetate-EDTA buffer, pH 8.5, TAE; L) Dulbecco phosphate buffered saline, DPBS.

Non-specific binding or non-specific adsorption of the 2^0Ab~QD molecules can increase the background signal and decrease the detection sensitivity. It can even lead to false positives or false negative results. To eliminate sources of false positives and false negatives as well as to optimize the system, blocking non-specific signals was studied using different buffers. To carry this process out, SK-BR3 cells were incubated with different concentrations of QDs at 37°C for 1 h with/without exposure to different blocking buffers. After the incubation process that allowed the QDs to non-specifically bind/attach on the cell surface and on the capture surface, as well as to allow non-specific uptake by exogenetic substrates, the sensor surfaces were washed to remove the excess QDs. The sensor surfaces were inspected under a fluorescence microscope. Optimized parameters were obtained to minimize the non-specific signals and the suitable blocking buffer was chosen for the succeeding processes.

To optimize the 2^0Ab~QD concentrations with the best cell imaging sensitivity, different concentrations of 2^0Ab~QD conjugates were used (0, 0.1, 0.5, and 1 nM). The concentration giving the best fluorescent image of the cells was established and used for the rest of the studies. Different concentrations of SK-BR3 cells (100,000 cells, 50,000 cells, 10,000 cells, 5,000 cells and 1,000 cells) were studied to establish the dynamic range of cell concentration that can be detected by the sensor.

3.8. Microscopy of the QD-based whole cell sensor

The glass slide solid phase QD-based whole cell sensor (complete and incomplete complexes) was observed under an Amscope UV-illuminated microscope (Ashford, United Kingdom). The glass slide solid phase sensor for whole cells were observed at 200 or 400 × magnifications and digital photographs were taken at various sections of the slide. The captured cells did not require additional treatments before microscope observations.

4. RESULTS AND DISSCUSSION

The complete QD-based whole cell sensor consisting of the aminoproyl triethoxy silanized glass slide~1^0Ab+SK-BR3 +Ab' + 2^0Ab~QD resulted in bright and stable fluorescent images. The incomplete complexes that lacked one or more of the components of the assay did not exhibit fluorescence after treatment with the blocking buffers.

4.1. Characterization of QDs and QD-antibody conjugates

The CdSe/ZnS core/shell QDs were characterized to establish the physical properties as well as the optical properties that were necessary to carry out the imaging sensor development. The size of the QDs after synthesis in organic solvent was established using TEM that exhibited the QDs at approximately 7 nm in diameter (Figure 2A) prior to the surface coating modification that was used for the conversion to water soluble form. The size was further confirmed with dynamic light scattering (DSL) shown in Figure 2A. After the QDs were converted into water soluble form using a triblock polymer coating (45), the diameter increased to approximately 16 nm. The zeta potential was recorded at -42.51 mV that may be attributed to the surface functionalization with carboxyl groups from the polymer coating. The surface coated water soluble CdSe/ZnS core/shell QDs exhibited the same optical properties as the original organic soluble form. In Figure 2B, the QDs showed a UV-vis absorption peak at around 610 nm with fluorescence emission at around 620 nm. The quantum yield of >50% was measured with the integrating sphere method.

The antibody conjugated QDs were also tested for changes in optical and physical properties. The DLS data indicated an increase in size to approximately 21 nm in diameter (Figure 2C) while the zeta potential decreased to -32.25 mV. The conjugation of antibodies onto the surface of QDs was further confirmed with agarose gel electrophoresis. The results shown in Figure 2D revealed that the carboxylated QDs had greater migration distances than the 2^0Ab~QD which were in agreement with their strongly negative zeta potential and smaller size. This indicated that the antibodies were attached to the QDs. Even when the 2^0Ab~QD conjugates were stored in buffers for several days, the fluorescence signal did not change compared with the original non-conjugated carboxyl

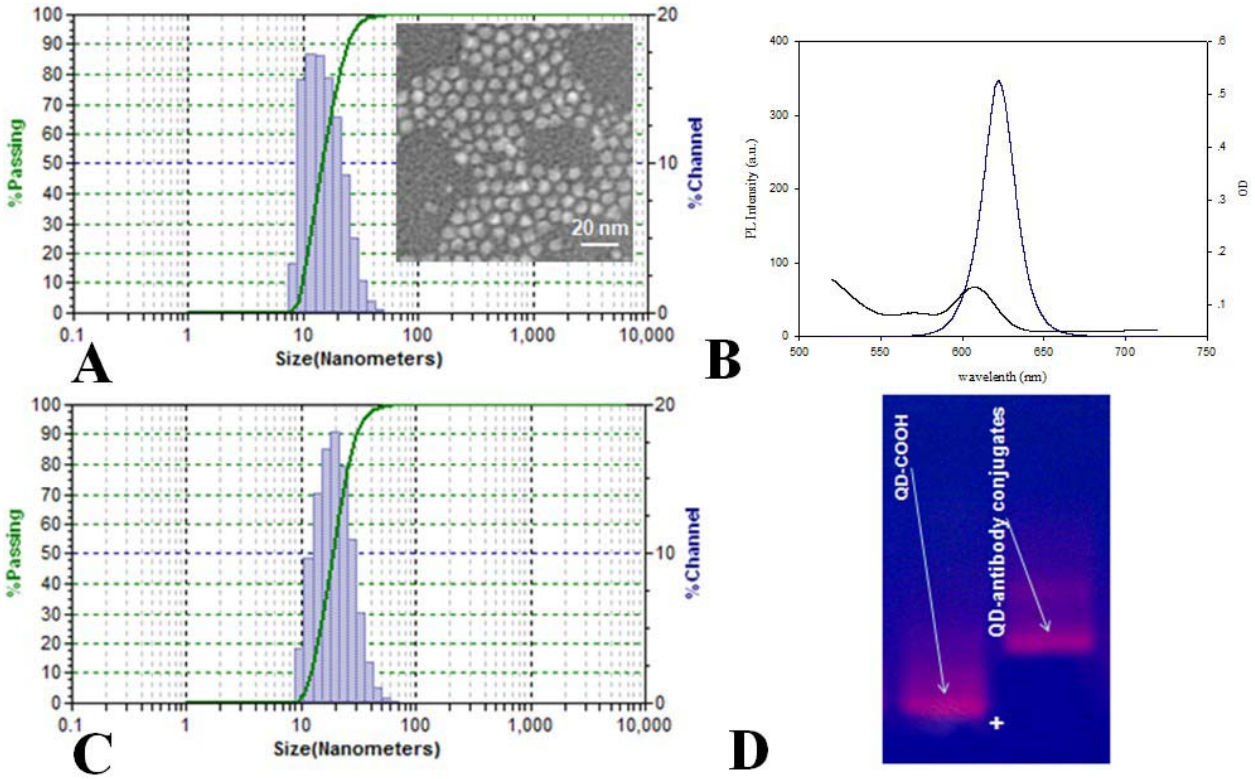

Figure 2. A) TEM image (right) of the CdSe/ZnS QDs inorganic core and hydrodynamic properties (left) of the original QDs before conversion into water soluble form, B) UV-vis absorption (black color curves) and fluorescence emission spectra (symmetric peaks at 625 nm) of QDs in water, C) hydrodynamic properties of the QD-antibody conjugates in water, and D) agarose gel electrophoresis of carboxyl terminated QDs (left lane) and QD-antibody conjugates (right lane), "+" indicates the positive pole.

functionalized QDs. This indicated strong fluorescence and stable properties of the 2^0Ab~QD conjugates.

4.2. Optimization and blocking of non-specific signals

Non-specific binding of the sensor molecules can increase the system background noise and decrease the detection sensitivity or even lead to false positives or false negative results. To optimize the model sensing system and to block non-specific signals, different buffers were tested. The results shown in Figure 4A-4B indicated that blocking buffer BBB eliminated the non-specific signals from the sensor surface. It is anticipated that the decrease in the non-specific binding was caused by the presence of blocker proteins and detergents in the blocking buffer. The detergents washed off adhering QDs and/or 2^0Ab~QD on the cell surface before these were attached and internalized through endocytosis. In our studies, this was not observed but in instances where the QDs were internally uptaken, the NSU may not be shed off after exposure to the blocking buffer. Proposed alternatives to eliminate non-specific binding of QDs that had been reported in the literature involved the modification of QD surfaces, pretreatment of target molecules, and decreased reaction temperature (46-50).

4.3. Optimization of the 2^0Ab~QD concentration

The components of the assay in a biosensor control the signals of the sensor. In order to make sure that the signals are dependent only on the amount of analyte present and not on other factors, the 2^0Ab~QD concentration was optimized to obtain the minimum amount that leads to the best fluorescent signal. As shown in Figure 4, the signals increased proportionately with the 2^0Ab~QD conjugate concentrations. At 1 nM concentration of 2^0Ab~QD conjugate, the brightest signal was obtained within the various concentrations tested. Thus, this concentration was used for all the succeeding studies.

Although the best signals were achieved at 1 nM 2^0Ab~QD concentration, the volume used was only 2 uL in 45 uL of cell suspension. Therefore, the absolute amount of 2^0Ab~QD used per sample was only 44 picomoles. This is very significant because quantum dots are very expensive and, therefore, the use of very small amounts can significantly reduce the cost of an assay.

4.4. Capture and detection of whole cells with 2^0Ab~QD conjugates

The QD-based whole cell biosensor was used for the detection of breast cancer cell line SK-BR3 that have over expressed Her2/neu and EpCAM antigen on the cell surface. As shown in Figure 5A, the breast cancer cells that were captured on glass slide in a complete sandwich type complex consisting of 1^0Ab+SK-BR3 +Ab' + 2^0Ab~QD were successfully immobilized and detected as red fluorescent cells. The cells appeared as bright red fluorescent round structures that corresponded to the cells

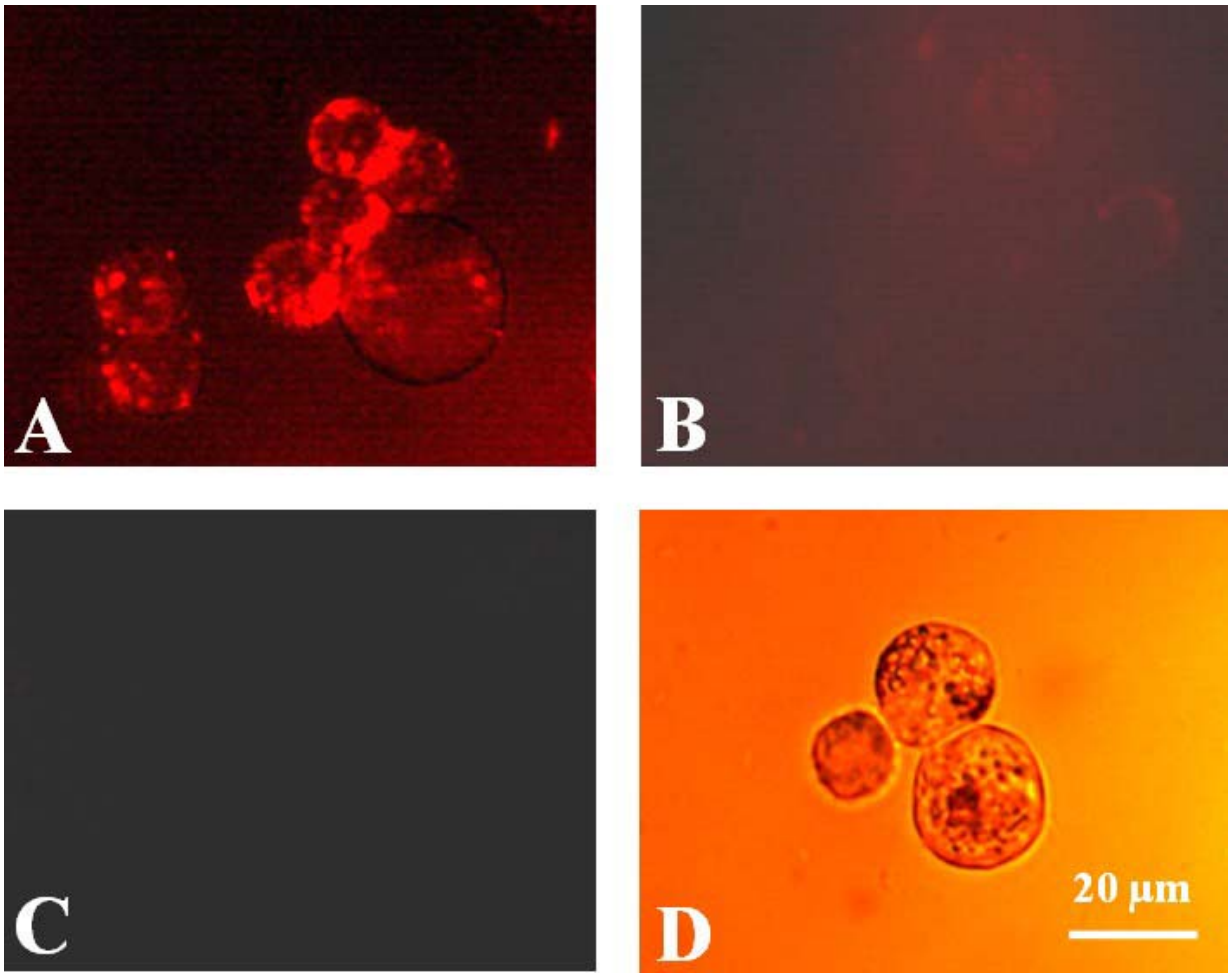

Figure 3. Non-specific cellular uptake/absorption of QDs and its elimination with blocking buffer. A 100,000 SK-BR3 cells tested with (A) 5 nM QDs without blocking, (B) 5 nM QDs h blocking with buffer BBB, (C) cells without exposure to QDs under white light and (D) UV light source.

observed under white light. It is deduced that the ring shaped red fluorescence indicated that most of the quantum dots were attached to the cell surface as a result of the presence of anti-EpCAM IgG (Ab') against the cancer cell surface protein EpCAM. EpCAM is a cell surface molecule that is highly expressed in colon and other epithelial carcinomas (51-53).

The antibody modified silanized capture area of about 10 mm^2 sufficiently immobilized the whole cells from a DPBS suspension. The solid phase immobilized cells were imaged after treatment with 2^0Ab~QD. The solid phase QD-based whole cell sensor was used to immobilized whole cells from 100,000 to 5,000 cells in DPBS suspension that were detected under a fluorescence microscope.

The SK-BR3 cells in the complete assay complex were stable under 4oC even after one week of storage. Majority of the cells kept their circular shape and bright red fluorescence resulting from the 20Ab~QD attachment. In comparison, the SK-BR3 cells in the 10Ab+SK-BR3 +Ab' + TexRed~20Ab complex shown in Figure 5B, had lighter coloration. Furthermore, the cells with TexRed~20Ab under the microscope lost their coloration resulting from photo bleaching after several hours under the microscope. In contrast, the QD-based cell detection did not show any change in fluorescence while under the microscope for several hours and even after storage for one week.

For sensitive and specific signals, antibodies are usually used for the specific capture of cells, biomolecules or microorganisms of interest that may be present in a complex sample. With optical transducers, a color-based assay is accomplished with enzyme-conjugated antibodies or dye conjugated antibodies. In a conventional assay, organic dyes are used but these are unstable and the signals decrease even during the observation process because of photo bleaching. In the present study, the use of QDs resulted in significantly enhanced signals in the detection of whole cells. The stability and high brightness of the QD-labeled cells resulted from the high emission intensity and high photo stability of the QDs compared with Texas red.

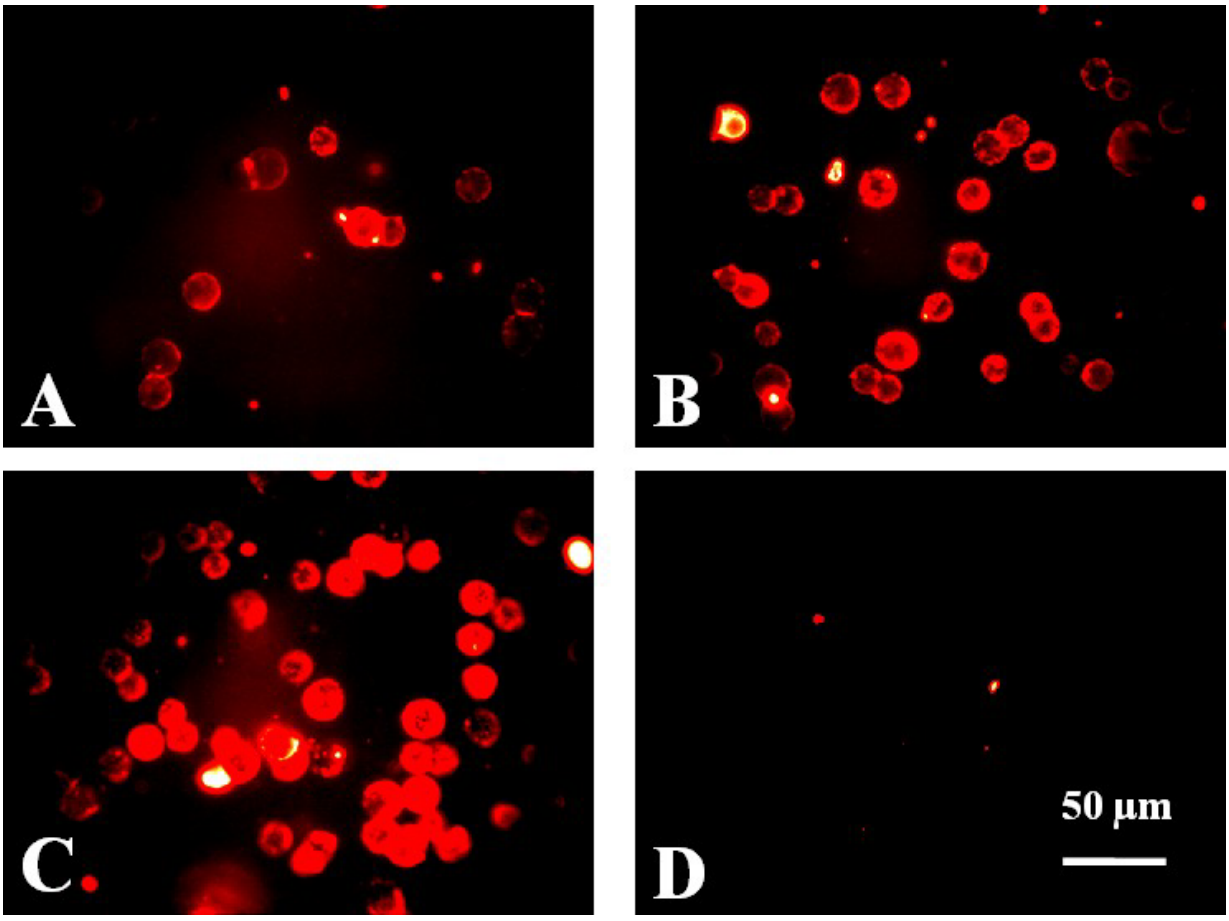

Figure 4. Effect of QD-antibody concentrations on the fluorescent detection of 100,000 SK-BR3 cells. (A) 0.1 nM, (B) 0.5 nM, (C) 1 nM QD-antibody conjugates and (D) control with 1 nM only QDs.

To establish the application of the QD-based whole cell sensor for quantitative detection of target cells, suspensions containing different number of cells were used. The results shown in Figure 6 indicated that the QD-labeled cells in a cell suspension containing 100,000 cells were distinguished from 50,000, 10,000, and 5,000 cells. The cell density and fluorescence brightness were observable under the microscope. This was done in triplicate analysis and similar results were obtained. Capture of the cells from the suspension onto the silanized and antibody modified glass slide immobilized the cells, thus showing a dense fluorescent population resulting from the use of 2^0Ab~QD. Fluorescent cell numbers based on a manual raster over the immobilization surface viewed under the microscope resulted in relevant cell numbers that corresponded to 100% for the 100,000 cell sample and 40%, 8%, 3% for the 50,000, 10,000 and 5000, respectively. However, cell number below 1000 was not detectable directly from the microscope using this system. This may because of the random distribution of the low cell population captured on the slide from the low cell concentration in suspension. Hence, we conclude that this system is good for as low as 5000 cells.

We have shown the use of QDs for the detection of whole cells in a silanized microscope glass slide using breast cancer cells as the model analyte. We believe this is the first report of whole cells immobilized on aminopropyl ethoxy silanized glass slide, labeled with specific antibodies, and detected with QD-antibody conjugates that targeted the labeling antibodies attached to surface proteins on the breast cancer cells forming the complete assay consisting of 1^0Ab + SK-BR3 + Ab' + 2^0Ab~QD. The complete assay resulted in fluorescent cells as seen under the microscope. Comparison of cell imaging with QDs against imaging with Texas red dye indicated that the cells with the QDs were 90% brighter. Furthermore, the QD imaged cells remained bright even after one week of storage indicating the stability of the QDs for imaging cells. Thus, semiconductor QD based biosensors hold promise for the sensitive and specific imaging and detection of whole cells.

5. CONCLUSION

We have successfully demonstrated a heterogeneous solid platform semiconductor nanomaterials-based whole cell biosensor using human breast cancer cell SK-BR3 as the model analyte. Capture and detection of the whole cells in a sandwich-type assay

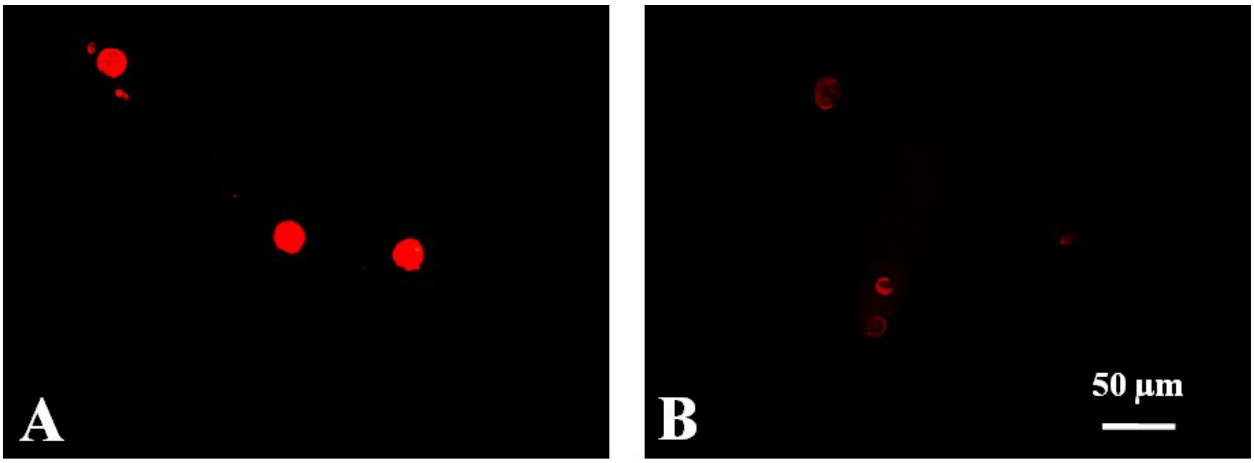

Figure 5. Digital photographs of microscope images of 10,000 breast cancer cells (SK-BR3) captured on antibody-modified silanized glass slide and imaged under UV light using A) QDs labeled antibodies and B) Texas red labeled antibodies for imaging.

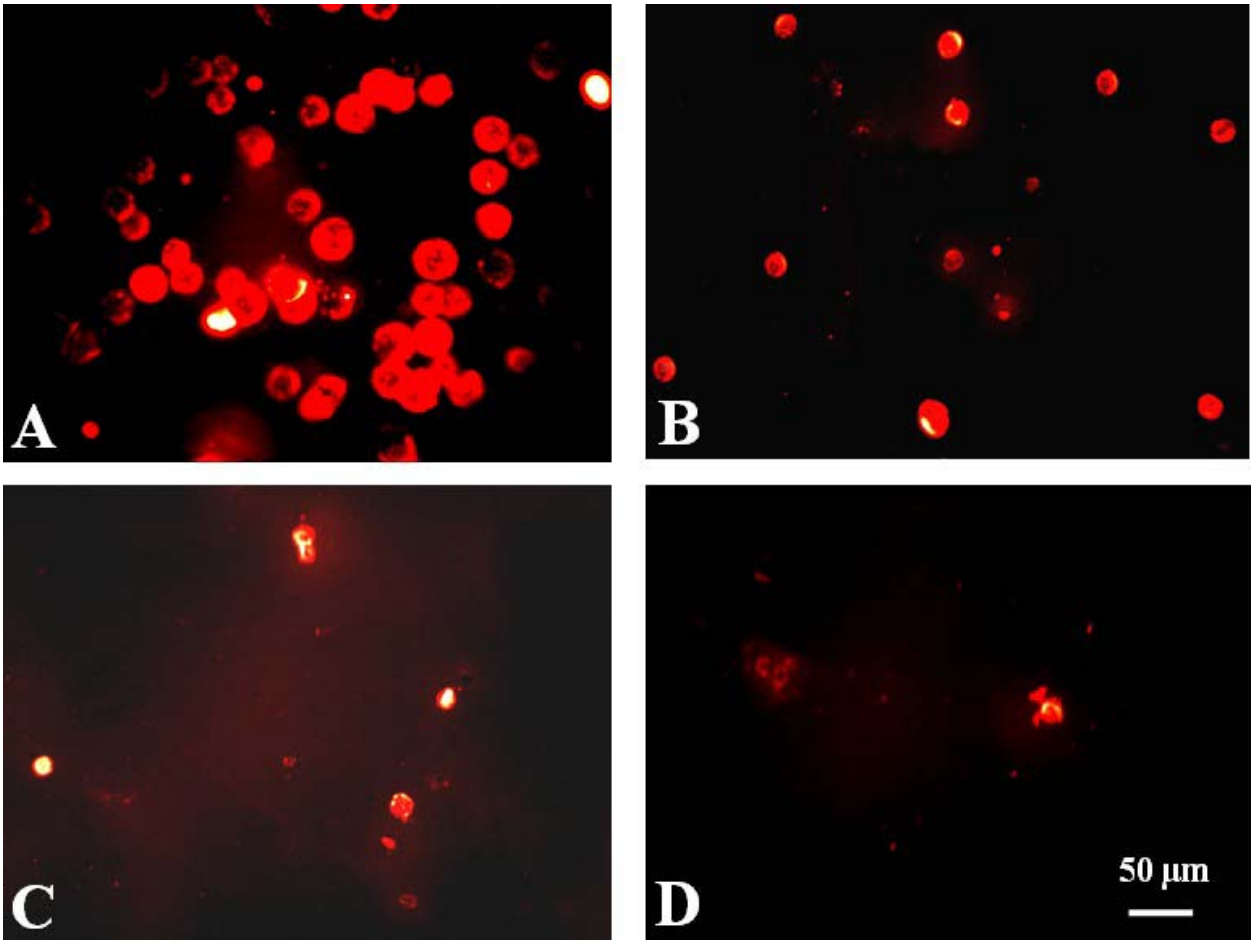

Figure 6. Digital photographs of microscope images of breast cancer cells (SK-BR3) captured on antibody-modified silanized glass slide and imaged under UV light with different sample cell numbers A) 100,000, B) 50,000, C) 10,000 and D) 5000 cells.

involved silanized microscope glass slides modified with monoclonal antibodies against EpCAM proteins that are found on the surface of the cells. To complete the sensor, quantum dot labeled antibodies were exposed to the assay complex. QDs emitting at 620 nm rendered the cells as bright red circular objects under UV-illuminated

microscope. The QDs based whole cell biosensor was stable even after storage for more than a week at 4°C. The assay involved only 44 picomoles of QDs that was used to detect as low as 5000 cells in an un-optimized system. The whole cell biosensor using semiconductor nanomaterials showed great promise for application in clinical diagnosis, environmental monitoring, food analysis, and other biological applications.

6. ACKNOWLEDGMENTS

This work was partly supported by a grant from National Science Foundation (NSF) and National Institute of Health (NIH). This work was also supported in part by a grant from "Cultivating the Excellent Ph. D Thesis of Jiangxi Province (YBP08A03)" of the Education Department of Jiangxi Province, China and the facilities at Ocean NanoTech in Springdale, AR, USA. The authors would like to thank Ocean NanoTech's technician Benjamin Jones for the picture drawing and John Dixon for purification of the QDs nanocrystals; University of Arkansas's REU students Joy Labayan, Chong Thor, and Debby Chou for cell counting and picture taking.

7. REFERENCES

1. S. Kumar & T. Nann: Shape control of II-VI semiconductor nanomaterials. *Small* 2, 316 (2006)

2. J. Ahn, H. Kim, K. Lee, S. Jeon, S. Kang, Y. Sun, R. Nuzzo & J. Rogers: Heterogeneous three-dimensional electronics by use of printed semiconductor nanomaterials. *Science* 314, 1754 (2006)

3. Y. Didenko & K. Suslick: Chemical aerosol flow synthesis of semiconductor nanoparticles. *J Am Chem Soc* 127, 12196-12197 (2005)

4. X. Michalet, F. Pinaud, L. Bentolila, J. Tsay, S. Doose, J. Li, G. Sundaresan, A. Wu, S. Gambhir & S. Weiss: Quantum dots for live cells, *in vivo* imaging, and diagnostics. *Science* 307, 538 (2005)

5. S. Courty, C. Luccardini, Y. Bellaiche, G. Cappello & M. Dahan: Tracking individual kinesin motors in living cells using single quantum-dot imaging. *Nano Lett* 6, 1491-1495 (2006)

6. B. Dubertret, P. Skourides, D. Norris, V. Noireaux, A. Brivanlou & A. Libchaber: *In vivo* imaging of quantum dots encapsulated in phospholipid micelles. *Science* 298, 1759 (2002)

7. B. Ballou, B. Lagerholm, L. Ernst, M. Bruchez & A. Waggoner: Noninvasive imaging of quantum dots in mice. *Bioconjugate Chem* 15, 79-86 (2004)

8. J. Tsay, S. Doose, F. Pinaud & S. Weiss: Enhancing the photoluminescence of peptide-coated nanocrystals with shell composition and UV irradiation. *J Phys Chem B* 109, 1669 (2005)

9. W. Guo, J. Li, Y. Wang & X. Peng: Luminescent CdSe/CdS core/shell nanocrystals in dendron boxes: superior chemical, photochemical and thermal stability. *J Am Chem Soc* 125, 3901-3909 (2003)

10. H. Mattoussi, J. Mauro, E. Goldman, G. Anderson, V. Sundar, F. Mikulec & M. Bawendi: Self-Assembly of CdSe- ZnS Quantum Dot Bioconjugates Using an Engineered Recombinant Protein. *J Am Chem Soc* 122, 12142-12150 (2000)

11. M. Daniel & D. Astruc: Gold nanoparticles: assembly, supramolecular chemistry, quantum-size-related properties, and applications toward biology, catalysis, and nanotechnology. *Chem Rev* 104, 293-346 (2004)

12. B. Dabbousi, J. Rodriguez-Viejo, F. Mikulec, J. Heine, H. Mattoussi, R. Ober, K. Jensen & M. Bawendi: (CdSe) ZnS Core- Shell Quantum Dots: Synthesis and Characterization of a Size Series of Highly Luminescent Nanocrystallites. *J Phys Chem B* 101, 9463-9475 (1997)

13. W. Chan & S. Nie: Quantum dot bioconjugates for ultrasensitive nonisotopic detection. *Science* 281, 2016 (1998)

14. Y. Xiao & P. Barker: Semiconductor nanocrystal probes for human metaphase chromosomes. *Nucleic Acids Res* 32, e28 (2004)

15. T. Lacoste, X. Michalet, F. Pinaud, D. Chemla, A. Alivisatos & S. Weiss: Ultrahigh-resolution multicolor colocalization of single fluorescent probes. *Proc Natl Acad Sci USA* 97, 9461 (2000)

16. F. Patolsky, R. Gill, Y. Weizmann, T. Mokari, U. Banin & I. Willner: Lighting-Up the Dynamics of Telomerization and DNA Replication by CdSe- ZnS Quantum Dots. *J Am Chem Soc* 125, 13918-13919 (2003)

17. F. Pinaud, D. King, H. Moore & S. Weiss: Bioactivation and cell targeting of semiconductor CdSe/ZnS nanocrystals with phytochelatin-related peptides. *J Am Chem Soc* 126, 6115-6123 (2004)

18. M. Bruchez Jr, M. Moronne, P. Gin, S. Weiss & A. Alivisatos: Semiconductor nanocrystals as fluorescent biological labels. *Science* 281, 2013-2016 (1998)

19. M. kerman, W. Chan, P. Laakkonen, S. Bhatia & E. Ruoslahti: Nanocrystal targeting *in vivo*. *Proc Natl Acad Sci USA* 99, 12617 (2002)

20. G. Mitchell, C. Mirkin & R. Letsinger: Programmed assembly of DNA functionalized quantum dots. *J Am Chem Soc* 121, 8122-8123 (1999)

21. E. Goldman, G. Anderson, P. Tran, H. Mattoussi, P. Charles & J. Mauro: Conjugation of luminescent quantum dots with antibodies using an engineered adaptor protein to provide new reagents for fluoroimmunoassays. *Anal Chem* 74, 841-847 (2002)

22. M. Dahan, S. Levi, C. Luccardini, P. Rostaing, B. Riveau & A. Triller: Diffusion dynamics of glycine receptors revealed by single-quantum dot tracking. *Science* 302, 442 (2003)

23. X. Wu, H. Liu, J. Liu, K. Haley, J. Treadway, J. Larson, N. Ge, F. Peale & M. Bruchez: Immunofluorescent labeling of cancer marker Her2 and other cellular targets with semiconductor quantum dots. *Nat Biotechnol* 21, 41-46 (2002)

24. J. Jaiswal, H. Mattoussi, J. Mauro & S. Simon: Long-term multiple color imaging of live cells using quantum dot bioconjugates. *Nat Biotechnol* 21, 47-51 (2002)

25. A. M nsson, M. Sundberg, M. Balaz, R. Bunk, I. Nicholls, P. Omling, S. T gerud & L. Montelius: *In vitro* sliding of actin filaments labelled with single quantum dots. *Biochem Biophys Res Commun* 314, 529-534 (2004)

26. J. Winter, T. Liu, B. Korgel & C. Schmidt: Recognition molecule directed interfacing between semiconductor quantum dots and nerve cells. *Adv Mater* 13, 1673-1677 (2001)

27. D. Lidke, P. Nagy, R. Heintzmann, D. Arndt-Jovin, J. Post, H. Grecco, E. Jares-Erijman & T. Jovin: Quantum dot ligands provide new insights into erbB/HER receptor¨Cmediated signal transduction. *Nat Biotechnol* 22, 198-203 (2004)

28. S. Rosenthal, I. Tomlinson, E. Adkins, S. Schroeter, S. Adams, L. Swafford, J. McBride, Y. Wang, L. DeFelice & R. Blakely: Targeting cell surface receptors with ligand-conjugated nanocrystals. *J Am Chem Soc* 124, 4586-4594 (2002)

29. A. Sukhanova, J. Devy, L. Venteo, H. Kaplan, M. Artemyev, V. Oleinikov, D. Klinov, M. Pluot, J. Cohen & I. Nabiev: Biocompatible fluorescent nanocrystals for immunolabeling of membrane proteins and cells. *Anal biochem* 324, 60-67 (2004)

30. F. Tokumasu & J. Dvorak: Development and application of quantum dots for immunocytochemistry of human erythrocytes. *J microscopy* 211, 256-261 (2003)

31. Xavier Michalet, Fabien Pinaud, Thilo D. Lacoste, Maxime Dahan, Marcel P. Bruchez, A. Paul Alivisatos & S. Weiss: Properties of fluorescent semiconductor nanocrystals and their application to biological labeling. *Single Mol* 2, 261-276 (2001)

32. S. Pathak, S. Choi, N. Arnheim & M. Thompson: Hydroxylated quantum dots as luminescent probes for *in situ* hybridization. *J Am Chem Soc* 123, 4103-4104 (2001)

33. J. Jaiswal, H. Mattoussi, J. Mauro & S. Simon: Long-term multiple color imaging of live cells using quantum dot bioconjugates. *Nat Biotechnol* 21, 47-51 (2003)

34. L. Mattheakis, J. Dias, Y. Choi, J. Gong, M. Bruchez, J. Liu & E. Wang: Optical coding of mammalian cells using semiconductor quantum dots. *Anal biochem* 327, 200-208 (2004)

35. T. Pellegrino, W. Parak & R. Boudreau: Quantum dot-based cell motility assay. *Differentiation* 71, 542-548 (2003)

36. Z. P. Aguilar, H. Xu, J. Dixon & A. Wang: Blocking Non-Specific Uptake of Engineered Nanomaterials. *ECS Trans* 25, 37-48 (2010)

37. H. Xu, Z. P. Aguilar & A. Wang: Quantum Dot-based Sensors for Proteins. *ECS Trans* 25, 1-8 (2010)

38. J. Kloepfer, R. Mielke, M. Wong, K. Nealson, G. Stucky & J. Nadeau: Quantum dots as strain-and metabolism-specific microbiological labels. *Appl Environ Microbiol* 69, 4205 (2003)

39. C. Dameron, R. Reese, R. Mehra, A. Kortan, P. Carroll, M. Steigerwald, L. Brus & D. Winge: Biosynthesis of cadmium sulphide quantum semiconductor crystallites. *Nature* 338, 596-597 (1989)

40. S. Whaley, D. English, E. Hu, P. Barbara & A. Belcher: Selection of peptides with semiconductor binding specificity for directed nanocrystal assembly. *Nature* 405, 665-668 (2000)

41. H. Bao, Y. Gong, Z. Li & M. Gao: Enhancement Effect of Illumination on the Photoluminescence of Water-Soluble CdTe Nanocrystals: Toward Highly Fluorescent CdTe/CdS Core- Shell Structure. *Chem Mater* 16, 3853-3859 (2004)

42. W. Mao, J. Guo, W. Yang, C. Wang, J. He & J. Chen: Synthesis of high-quality near-infrared-emitting CdTeS alloyed quantum dots via the hydrothermal method. *Nanotechnology* 18, 485611 (2007)

43. J. Merlin, M. Barberi-Heyob & N. Bachmann: *In vitro* comparative evaluation of trastuzumab (Herceptin (R)) combined with paclitaxel (Taxol (R)) or docetaxel (Taxotere (R)) in HER2-expressing human breast cancer cell lines. *Ann Oncol* 13, 1743 (2002)

44. J. Menendez, L. Vellon, I. Mehmi, B. Oza, S. Ropero, R. Colomer & R. Lupu: Inhibition of fatty acid synthase (FAS) suppresses HER2/neu (erbB-2) oncogene overexpression in cancer cells. *Proc Natl Acad Sci USA* 101, 10715 (2004)

45. K. Chen, J. Xie, H. Xu, D. Behera, M. H. Michalski, S. Biswal, A. Wang & X. Chen: Triblock copolymer coated iron oxide nanoparticle conjugate for tumor integrin targeting. *Biomaterials* 30, 6912-6919 (2009)

46. M. Mancini, B. Kairdolf, A. Smith & S. Nie: Oxidative quenching and degradation of polymer-encapsulated quantum dots: new insights into the long-term fate and toxicity of nanocrystals *in vivo*. *J Am Chem Soc* 130, 10836-10837 (2008)

47. E. Bentzen, I. Tomlinson, J. Mason, P. Gresch, M. Warnement, D. Wright, E. Sanders-Bush, R. Blakely & S. Rosenthal: Surface modification to reduce nonspecific

binding of quantum dots in live cell assays. *Bioconjugate Chem* 16, 1488-1494 (2005)

48. R. Mahtab, H. Harden & C. Murphy: Temperature-and Salt-Dependent Binding of Long DNA to Protein-Sized Quantum Dots: Thermodynamics of "Inorganic Protein"-DNA Interactions. *J Am Chem Soc* 122, 14-17 (2000)

49. M. Yezhelyev, X. Gao, Y. Xing, A. Al-Hajj, S. Nie & R. O'Regan: Emerging use of nanoparticles in diagnosis and treatment of breast cancer. *Lancet Oncol* 7, 657-667 (2006)

50. B. A. Kairdolf, M. C. Mancini, A. M. Smith & S. Nie: Minimizing Nonspecific Cellular Binding of Quantum Dots with Hydroxyl-Derivatized Surface Coatings. *Anal Chem* 80, 3029-3034 (2008)

51. W. Osta, Y. Chen, K. Mikhitarian, M. Mitas, M. Salem, Y. Hannun, D. Cole & W. Gillanders: EpCAM is overexpressed in breast cancer and is a potential target for breast cancer gene therapy. *Cancer Res* 64, 5818 (2004)

52. C. Hough, C. Sherman-Baust, E. Pizer, F. Montz, D. Im, N. Rosenshein, K. Cho, G. Riggins & P. Morin: Large-scale serial analysis of gene expression reveals genes differentially expressed in ovarian cancer. *Cancer Res* 60, 6281 (2000)

53. P. Went, A. Lugli, S. Meier, M. Bundi, M. Mirlacher, G. Sauter & S. Dirnhofer: Frequent EpCam protein expression in human carcinomas. *Human pathology* 35, 122-128 (2004)

Key Words: Quantum Dots, QDs, Whole Cell, Cell, Semiconductor Nanomaterials, Biosensor

Send correspondence to: Hua Wei, State Key Laboratory of Food Science and Technology, Jiangxi-OAI Joint Research Institute, Nanchang University, Nanchang 330047, China. Tel: 0086-791-833-4578, Fax: 0086-791-833-3708, E-mail: hua_wei114@yahoo.com.cn

http://www.bioscience.org/current/volE3.htm